Genome Biology

Genome Biology
Biology for the post-genomic era

Consistent dissection of the protein interaction network by combining global and local metrics

Genome Biology 2007, **8**:R271 doi:10.1186/gb-2007-8-12-r271

Chunlin Wang (wangcl@stanford.edu)
Chris Ding (chqding@lbl.gov)
Qiaofeng Yang (qyang@lbl.gov)
Stephen R Holbrook (SRHolbrook@lbl.gov)

ISSN 1465-6906

Article type Method

Submission date 22 June 2007

Acceptance date 21 December 2007

Publication date 21 December 2007

Article URL http://genomebiology.com/2007/8/12/R271

Consistent Dissection of the Protein Interaction Network by Combining Global and Local Metrics

Chunlin Wang[1,3§], Chris Ding[2], Qiaofeng Yang[1], Stephen R. Holbrook[1§]

[1]Physical Biosciences Division, Lawrence Berkeley National Laboratory, Berkeley, CA 94720, USA.

[2]Computational Research Division, Lawrence Berkeley National Laboratory, Berkeley, CA 94720, USA

[3]Present address: Division of Infectious Diseases, School of Medicine, Stanford University, Stanford, CA 94035, USA

[§]Corresponding author

Email addresses:

CLW: wangcl@stanford.edu

CD: CHQDing@lbl.gov

QFY: QYang@lbl.gov

SRH: SRHolbrook@lbl.gov

Abstract

We propose a new network decomposition method to systematically identify protein interaction modules in the protein interaction network. Our method incorporates both a global metric and a local metric for balance and consistency. We have compared the performance of our method with several earlier approaches on both simulated and real datasets using different criteria, and show that our method is more robust to network alterations and more effective at discovering functional protein modules.

Background

Protein complexes are building blocks of cellular components and pathways. A comprehensive understanding of a biological system requires knowledge about how protein complexes are assembled, regulated, and organized to form cellular components and perform cellular functions. The emergence of a variety of genomic and proteomic techniques to systematically obtain such information has generated an enormous amount of data [1-11]. However, interpretation and analysis of such data in terms of biological function has not kept pace with data acquisition, mainly due to the complexity of the problem and the limitation of current techniques to handle the data.

In this paper, we address the issue of constructing protein interaction modules from the protein interaction data. Highly connected protein modules are mostly found to be protein complexes performing a specific biological function. The concept of protein interaction modules as fundamental functional units was first outlined by Hartwell et al [12]. Protein interaction modules are composed of a variable number of proteins, with discrete functions arising from their individual constituents and their synergistic interactions. A

multi-protein complex, such as the ribosome, is one common form of interaction module; other examples of protein functional modules include proteins working collectively in a pathway, such as signal transduction, that do not necessarily form a tightly associated, stable protein complex.

To detect protein interaction modules from protein interaction data, we use a graph theory approach. Protein interaction networks are routinely represented as graphs, with proteins as nodes and interactions as edges. In a graphical representation of a protein interaction network, a functional unit, or a group of functionally related proteins, is tightly connected as a community, while proteins from different functional units are more loosely connected. In the past few years, new algorithms have been developed to extract communities from a generic network. Girvan & Newman [13] proposed a decomposition algorithm (GN algorithm) to analyze community structure in networks. Their algorithm iteratively removes edges based on betweenness values -- the number of shortest paths between all pairs of nodes in the network running through an edge, in contrast to the traditional hierarchical clustering algorithm where closely connected nodes are iteratively joined together into larger and larger communities. In a different approach, Radicchi et al. [14] replaced the edge betweenness metric with an edge clustering coefficient -- the number of triangles to which a given edge belongs, divided by the number of triangles that might potentially include it, given the degrees of the adjacent nodes. The edge clustering coefficient is a local topology-based metric and a candidate edge with the lowest clustering coefficient is removed one at a time in the algorithm of Radicchi et al ('edge clustering coefficient' algorithm, ECC algorithm for short).

When applied to a large network, these two algorithms give substantially different results. The reason is that an individual edge with larger betweenness does not necessarily have a lower clustering coefficient, although on average it will. Ultimately, the global metric in the GN algorithm behaves differently from the local metric in the ECC algorithm. In this paper, we propose to resolve this conflict by combining the global and local metrics to form a consistent and robust algorithm. We make three additional significant contributions: (1) a new metric (commonality) that takes into account the effects of random edge distributions; (2) a new definition of a protein interaction module; and (3) a novel filtering procedure to remove false-positive interactions based on a random graph model analysis. We demonstrate that our new algorithm is more effective and robust in terms of discovering protein interaction modules in protein interaction networks than either the global or local algorithm by application to the large yeast protein interaction network.

Results and Discussion

The principal result of this paper is the development of a new algorithm for extracting protein interaction modules from a protein interaction network. We first present the new methodology developments and then compare the performance of different algorithms, including the MCL algorithm [15], on simulated networks where protein complexes were known. The MCL algorithm is a fast and scalable unsupervised cluster algorithm for graphs based on simulation of stochastic flow in graphs [15] and was found to be overall the best performing one by the van Helden study [16]. Note that our proposed new algorithm, the GN algorithm, and the ECC algorithm are divisive partitioning-type

algorithms, while the MCL algorithm is a non-partitioning algorithm. Both the modularity [17] measure and productive cuts in the following sections are not applicable to the MCL algorithm. Second, we compare the results of different algorithms on a small protein interaction network where protein complexes are largely known. Lastly, we apply our new algorithm, the GN algorithm, the ECC algorithm, and the MCL algorithm whenever applicable, on two large yeast protein interaction networks and evaluated the performance of each algorithm based on the value of modularity [17], overlap with MIPS complexes [18] and Gene Ontology (GO, http://www.geneontology.org) term enrichment of each cluster.

A new commonality metric

Consider two proteins A and B. Let *k* be the number of common interacting partners (or neighbors) between A and B. If A and B belong to the same protein complex, they likely share many common interaction partners, i.e., have a large *k*. On the other hand, if A and B do not belong to the same protein complex, they likely have few common interaction partners, i.e., have a small *k*. However, randomness also enters the equation. Let n, m be the number of total interacting partners for protein A and B respectively (n and m are also called degrees of A and B). A standard model of a protein interaction type network is the fixed-degree-sequence random graph [19] where the interactions follow the hypergeometric distribution. From this model, the average number of common interacting partners between proteins A and B in a random graph is given by $\langle k \rangle = \frac{n \cdot m}{N}$ (N is the total number of nodes). To offset this random effect that a large k results from large n and

m, we propose a new commonality index as: $\frac{k+1}{\sqrt{n \cdot m}}$. The square root of $n \cdot m$ makes it a scale invariant. We note that in [14], the authors define a similar metric as: $\frac{k+1}{\min(n-1, m-1)}$.

BCD algorithm

Our goal is to discover protein interaction modules. Intuitively, when two protein functional modules are sparsely connected, edges between them should have higher edge-betweenness values and lower commonality, whereas edges within a module should have high commonality and low edge-betweeness. Thus for sparsely connected functional modules, edge-betweenness highly correlates with edge-commonality. When protein functional modules overlap, the correlation between the global metric and local metric becomes less clear. For this reason, we combine these two metrics to build a more consistent and robust metric. The new BCD (Betweenness-Commonality Decomposition) algorithm is summarized as follows:

1. Calculate the edge commonality (**C**) for each edge in the network.

2. Calculate the edge-betweenness (**B**) for each edge in the current subnetwork.

3. Remove the edge with the maximal ratio B/C.

4. Repeat steps 2 and 3 until no edges remain.

Like the edge clustering coefficient in the ECC algorithm, the edge commonality is a static property of an edge in context of the entire network, telling how strong the affinity

is between two nodes it connects. The edge commonality is calculated only once at the beginning of a decomposition process, while the edge-betweenness is updated each time an edge is removed to achieve best results [13]. This algorithm runs with $O(M^2N)$ computational complexity, where M is the number of edges and N is the number of nodes in a network. As a practical matter, we calculate the betweenness using the fast algorithm of Brandes [20] where the edge-betweenness value can be obtained by summing pair-dependencies over all traversals [21], so that we can easily parallelize the computationally costly betweenness calculation.

A new definition of protein interaction module

Intuitively, a protein interaction module is a subnetwork in the protein interaction network with more internal interactions than external interactions. A precise definition of the interaction module is not trivial. A number of definitions of community (or protein interaction module in terms of the protein interaction network) have been proposed with different criteria [14, 17, 22]. No clear consensus of module definition exists.

All three algorithms (BCD, GN, ECC) in this study transform a network into a decomposition tree (Figure 1). In this tree (called a dendrogram in the social sciences), the leaves are the nodes, whereas the branches join nodes or (at higher level) groups of nodes, thus identifying a hierarchical structure of communities nested within each other. When inspecting the resultant tree from either one of the tree algorithms on a small yeast transcription network with 225 proteins and 1,792 interactions, where known protein interaction modules can be inferred from the annotations of well-studied proteins, we found most, if not all, protein complexes, within which proteins are tightly grouped as

subtrees in the decomposition tree with uniform structure similar to those shadowed subtrees in Figure 1. Similar results were seen in much larger networks. Based on those observations, we propose a precise definition of a protein interaction module utilizing the decomposition tree structure. We first note that on the decomposition tree, all leaf nodes are single proteins, while non-leaf nodes are collections of proteins. We define a *special parent* as a non-leaf node with at least one child being a leaf (Figure 1). *A protein interaction module is then defined as the nodes of a maximal sub-tree where all non-leaf nodes are special parents.* Further, when two modules share the same parent, we merge them (see Figure 1, subtrees in solid boxes) when the maximal commonality of edges connecting these two modules is larger than a pre-defined cutoff. Currently, the cutoff is set at 0.1 to avoid merging two modules with very limited connections between them. Results on actual protein interaction networks indicate that proteins within a module as defined above have very similar GO (Genome Ontology) terms and perform similar functions (see Figure 3 for examples). The dangling nodes outside modules (in dashed boxes in Figure 1) are simply categorized as singletons.

Filtering false-positive interactions

Most yeast protein interaction data were obtained from large-scale, high-throughput experiments, which generally contain false positives [23]. To minimize the number of false positive interactions, we apply a statistical test to measure the reliability of an interaction (edge). We rigorously calculate the statistical significance of each interaction between two proteins as the random probability (*P*-value) that the number of common interacting partners occurs at or above the observed number. Previous work has shown

that the statistical significance based on the number of common interacting partners highly correlates with the functional association of two proteins [24, 25].

In a species with N proteins, the number of distinct ways in which two interacting proteins A and B with n and m interaction partners have k partners in common is given by $C_k^{N-2} \cdot C_{n-k-1}^{N-2-k} \cdot C_{m-k-1}^{N-n-1}$. The first factor ($C_k^{N-2}$) is the number of ways to choose the k common partners from all N proteins except proteins A and B. The second term (C_{n-k-1}^{N-2-k}) counts the number of ways of choosing dangling partners of protein A (Note that the common partners and protein A, B are excluded). Similarly, the third term (C_{m-k-1}^{N-n-1}) is for choosing dangling partners of protein B. The total number of ways for the two interacting proteins to have n and m interaction partners, regardless of how many are in common, is given by $C_{n-1}^{N-2} \cdot C_{m-1}^{N-2}$. Therefore, the probability to randomly see two interacting proteins with n and m partners, sharing k common partners in a species with N proteins is given by: $p(k \mid -, n, m, N) = \frac{C_k^{N-2} \cdot C_{n-k-1}^{N-2-k} \cdot C_{m-k-1}^{N-n-1}}{C_{n-1}^{N-2} \cdot C_{m-1}^{N-2}}$. The statistical significance is then calculated by $P = \sum_{k=k_0}^{\min(n-1,m-1)} p(k \mid -, n, m, N)$ where k_0 is the observed number of common partners shared by two interacting proteins. An interaction with *P*-value greater than 0.01 is considered to be a 'false-positive' and is discarded. We remove the edge with the highest *P*-value and recalculate the *P*-value for affected edges. The process is repeated until no edge has a *P*-value > 0.01. We found in analysis of yeast data, this filtering always improves the quality of discovered protein interaction modules.

Application to simulated yeast protein interaction networks

To compare the performance of our BCD algorithm, the GN algorithm, the ECC algorithm with the original edge clustering coefficient definition (ECC1), and the ECC algorithm with our commonality metric (ECC2), and the MCL algorithm [15], in which the inflation parameter was set to the optimal value 1.8 according to the study [16], we built a test graph on the basis of 198 complexes manually annotated in the MIPS database [18] in a way similar to that used in Brohee and van Helden's study [16]. Briefly, for each manually annotated MIPS complex, an edge was created between each pair of proteins within that complex. The resulting graph (referred to as test graph) contains 1078 proteins and 9919 interactions. To evaluate the robustness to false positives and false negatives, we derived 16 altered networks by randomly removing edges from or adding edges to the test graph in various proportions. We then assessed the quality of clustering results on each derived network by different algorithms with each annotated complex. As done in Brohee and van Helden's study [16], we computed a geometric accuracy value and a separation value to estimate the overall correspondence between a clustering result (a set of clusters) and the collection of annotated complexes, where both a high geometric accuracy value and a high separation value indicate good clustering (please check the reference [16] by Brohee and van Helden for more details).

Figure 2A displays the impact of edge addition on geometric accuracy and Figure 2B show the impact on separation. Clearly, the ECC2 algorithm with our new commonality metric greatly outperforms the ECC1 algorithm with the older edge clustering coefficient measure when the graph is altered with adding edges. In Figure 2C and 2D, increasing proportions (0%, 20% 40%, 60%, and 80%) of edges are randomly removed from the test

graph with prior 100% edge addition. Figure 2E and 2F show the effect of edge addition on graphs from which 40% of the edges had previously been removed. All curves show similar trends and that BCD and MCL outperform the other three algorithms. The performance of our BCD algorithm is better than that of the MCL algorithm when the graph is more dramatically altered with both edge removal and addition (Figure 2C-F).

Application to the yeast protein interaction network

We used the yeast protein interaction network from the BioGrid database (version 2.0.24) [26], from which we extracted 36,238 unique interactions among 5,273 yeast proteins. We applied the filtering process to the data and the resulting dataset retained 3,030 yeast proteins and 17,242 high-confidence interactions, which we call the filtered dataset. On both the original and filtered datasets, we tested five algorithms: (1) our BCD algorithm, (2) the GN algorithm, (3) the ECC1 algorithm with its original edge clustering coefficient, (4) the ECC2 algorithm with our commonality metric and (5) the MCL algorithm whenever applicable.

Results on a small yeast protein interaction network. Before diving into the entire complex network, we first decomposed a small yeast transcription network with 225 proteins and 1,792 interactions, where known protein interaction modules can be inferred from the annotations of well-studied proteins (Figure 3A). Figure 3B displays a hierarchical decomposition tree by the BCD algorithm (decomposition trees constructed by the other three algorithms are provided in Supplementary materials). Note that there is no decomposition tree for the MCL algorithm.

The proposed definition of protein interaction module works well for both the GN and BCD algorithms because almost all proteins within the same computed protein module do indeed belong to the same known protein complex. Decomposition trees obtained using the ECC1 algorithm and the ECC2 algorithm with our commonality metric are shown in Figure 1 of the Supplementary material. They produce irregularly large modules and an excess number of singletons (shown in Supplementary material). This suggests that the purely local metric used in the ECC algorithm is not effective. Figure. 1 in the Supplementary material also shows good results for both the GN and BCD algorithms that combine global and local metrics. They clearly produce more consistent and robust results.

The BCD algorithm revealed 21 functional modules (see Figure 3); all proteins within known protein complexes are also located within the same module, suggesting that the BCD algorithm is superior at unveiling fine structure buried in complex protein interaction networks. The MCL algorithm predicts only 11 clusters from this small yeast transcription network. Several functional modules are grouped together: 1) the three RNA dependent RNA polymerases (A, B, C) and the RNA polymerase II mediator complex are merged into one cluster; 2) the NuA4 histone acetyltransferase complex, the SWR1 complex, and the INO80 chromatin remodeling complex are grouped into one cluster; 3) the TFIIA complex, the Elongator complex, the SAGA histone acetyltransferase complex, and the TFIID complex are grouped into one cluster; and 4) the COMPASS complex and the mRNA cleavage and polyadenylation specificity complex (CPF) are grouped into one cluster. Apparently, the MCL algorithm is inefficient in discovering boundaries between functionally related protein complexes and tends to group them

together. The quality of modules obtained using the GN algorithm is not as good; members of four functional modules, transcription factor IIA (TFIIA) [TOA1, TOA2], TFIID [TAF2, TAF3, TAF4, TAF7, TAF8, TAF11, TAF13], nuclear pore-associated [SAC3, CDC31, THP1], and a new one [ABD1, SPT6] predicted by the BCD algorithm, are misplaced. The ECC algorithm has the same tendency to separate peripheral members of the same known protein complex into incorrect protein modules. For instance, in the transcription network, the ECC algorithm disjoins peripheral proteins such as FOB1, RPC10, RRP8 and RPL6B in a very early phase of the decomposition process, causing those derived singletons to be separated from most functional modules. Singletons don't provide useful information for inferring the function of any module. Therefore, the number of singletons generated by an algorithm is an additional indicator of that algorithm's performance: an excess number of singletons indicates poor performance of a particular algorithm. On this small network, the ECC algorithm produces 13 singletons, while the BCD and GN algorithms produce 9 and 3 singletons, respectively. While the difference between the ECC algorithm and the BCD algorithm is only 4 singletons, those ECC singletons lose their connections with other modules as they are isolated at a much earlier stage of the decomposition process. Although the GN algorithm produces the least number of singletons in the example network, it is at the expense of generating mosaic modules. Similar trends are seen in following experiments of large networks.

We also note that the original ECC1 algorithm performs more poorly than the ECC2 algorithm with our commonality index (see Figure 1 in Supplementary material). From now on, we will not discuss the original ECC1 algorithm. When we refer to the ECC algorithm, we mean the ECC algorithm using our commonality index.

Results on the global yeast network. In this section, we discuss the results of BCD decomposition of a specific network (yeast), the quality of computed modules, and comparison to MIPS hand-curated protein complex data.

We first studied the decomposition processes by the three algorithms as curves in Figure 4. Each curve displays the size of the current network on which an algorithm acts versus the number of productive cuts thus far. We consider the tendency of network fragmentation due to different algorithms, as measured by the number of productive cuts. Note that most module (complex) finding algorithms are typically applied on connected components of network. *A productive cut is defined as a removal of an edge resulting in two separate subnetworks.* On the original dataset, the BCD, GN and ECC algorithms require 674, 2,779, and 2,304 productive cuts to split the largest connected component of 5,257 nodes into smaller pieces, which means, on average, the algorithms separate 7.8, 1.9 and 2.3 nodes, respectively, from the largest connected component in each productive cut. On the filtered dataset, the respective algorithms require 80, 107 and 710 productive cuts, to split the largest connected component of 2,924 nodes into smaller pieces, which means, on average, the algorithms separate 36.5, 27.3 and 4.1 nodes, respectively, from the largest connected component in each productive cut. The more productive cuts made, the more fragmented the network and the more singletons generated as shown in Table 1. As stated earlier, a large number of singletons is an indicator of poor performance by a particular algorithm. For both datasets, the BCD algorithm produces the fewest singletons of the three partitioning-type algorithms. The size distributions of predicted protein complexes for each algorithm including the MCL algorithm on both datasets are shown in Figure 5. The pattern of predicted complexes generated by all three methods is similar

to that of hand-curated MIPS complexes [18], suggesting that the proposed protein module definition is effective.

Modularity. As a measure of the quality of the protein modules computed, we use modularity (Q) [17], which is a measure of a community structure in a network, measuring the difference between the number of edges falling within groups and the expected number in an equivalent network with edges placed at random. Basically, the higher the modularity, the better the separation. The best clusters are given at the point when the modularity is maximal. Previous studies stopped the decomposition process when the modularity reached its peak value and treated all resulting clusters as communities [17, 21]. Applying the modularity criteria on protein interaction networks in this study, however, we found that protein modules obtained in this way tend to be dominated by several very large examples. Nonetheless, the maximal modularity is an objective measure, which is useful for comparing the performance of different algorithms. Table 2 lists the maximal modularities obtained by three algorithms on three networks of different size. The BCD algorithm has the highest Q values for both the transcription network and the unfiltered global network and is very close to the highest Q value of the GN algorithm on the filtered data, suggesting that the BCD algorithm is best in terms of maximal modularity. In particular, on the noisy original data, the maximal modularity Q value by the BCD algorithm is significantly higher than the Q values by the other two algorithms, suggesting the tolerance of data noise by the BCD algorithm is much better than the other algorithms.

Overlap with MIPS complexes. We validated the biological significance of our predicted protein modules by comparing the hand-curated protein complexes in the MIPS

[27] database with the predicted modules. For each predicted module, we found a best-matching MIPS complex using Spirin's method [22], which finds two complexes with the least probability of random overlap using the hypergeometric distribution: $P_{overlap} = \frac{\binom{n}{k}\binom{N-n}{m-k}}{\binom{N}{m}}$, where N is the total number in the protein interaction network, n and m are the sizes of two complexes, and k is the number of common nodes. Table 3 presents the overlap (the number of common proteins divided by the number of proteins in the best-matching MIPS complexes) between predicted and MIPS complexes. In terms of the absolute number of clusters that overlap 100% with MIPS complexes, the BCD is the best one on the unfiltered dataset, while the MCL algorithm is the best on the filtered dataset. In terms of the percentage of clusters that overlap 100% with MIPS complexes, the MCL algorithm always performs better than the other three. However, we found the size of predicted clusters might affect the number. The larger a cluster is, the more likely it contains all members of an overlapping MIPS complex. From both Table 1 and Figure 5, the MCL algorithm produces a greater number of larger clusters than the other three algorithms, which was seen previously in the small yeast transcription network.

Therefore, to estimate the overall correspondence between a resulting cluster by one approach and the collection of annotated complexes, we computed the geometric accuracy and separation as done in the described study [16]. The results are shown in Table 3. Clearly, the BCD algorithm achieves better accuracy than the other three algorithms on both unfiltered and filtered datasets. In term of separation, it is the MCL algorithm that performs best among the four algorithms on both datasets (Table 3).

GO term enrichment. In addition to the MIPS protein complex dataset we also evaluated the biological significance of predicted protein modules by quantifying GO term co-occurrences using the SGD GO Term Finder [28]. The GO Term Finder calculates a P-value that reflects the probability of observing by chance the co-occurrence of proteins with a given GO annotation in a certain complex based on a binomial distribution. The lower the P-value of a GO term, the more statistically significant a complex is enriched in the GO term. Table 4 lists the percentage of predicted protein modules, whose P-value falls within $P <$ e-15, [e-15, e-10], [e-10, e-5] and [e-5, 1]. There are more BCD complexes in terms of absolute number, with P-value less than 1e-15 on both the unfiltered and filtered datasets.

Prediction of possible novel protein complexes. The number of predicted protein complexes is larger than the number of known protein complexes compiled in the MIPS complexes dataset, and many predicted protein complexes don't overlap with MIPS complexes. Among these unmatched predicted protein complexes, some are likely to be true functional protein modules because the GO terms in these complexes are greatly enriched as indicated by low P-values. Figure 6 presents two such modules: a five-member module (P=1.9e-12) of a spindle-assembly checkpoint complex that is crucial in the checkpoint mechanism required to prevent cell cycle progression into anaphase in the presence of spindle damage [29] (Figure 6A), and a thirteen-member module (P=9.8e-17) including members (Set3, Hos2, Snt1, Hos4, Hst1, Sif2) from the Set3 histone deacetylase complex [30], proteins (Zds1, Zds2 and Skg6) involved in telomeric silencing [31], proteins (Spr6 and Bem3) related to sporulation [32, 33] and two other

proteins (YIL055C and Cpr1) (Figure 6B). A complete list of complexes and modules with functional annotation is provided in the Supplementary Material.

Table 5 provides the number of predicted protein modules (4 algorithms, 2 datasets) where either the GO terms are greatly enriched (P<1e-15) or they overlap with MIPS complexes (overlap=100%). Generally, the protein modules falling within the above two categories can be viewed as functional modules. The BCD algorithm outperforms the other three algorithms in terms of identifying more functional protein modules on the unfiltered dataset. The MCL algorithm predicts more functional protein modules than our BCD algorithm does on the filtered dataset. In addition, all four algorithms predict a substantial number of complexes that don't overlap with MIPS or in which GO term co-occurrences are insignificant. However, these are potentially novel functional complexes for biologists to further explore.

The effects of filtering false-positive interactions. In all experiments, the results on the filtered data are consistently better than the results on the original data. For example in Table 3, the non-overlap between computed protein modules by the BCD algorithm and known protein complexes was reduced from 601 for the original data to 209 on the filtered data. In Table 4, the percentage of GO terms with probability < e-10 is always higher in the filtered data than in the original data.

Discussion

Protein interaction networks are examples of complex systems that are difficult to understand from raw experimental data alone. Methods to organize, filter, extract significant features and display these data are critical to understanding these systems. A

number of network partition algorithms have been proposed to find modular structures in protein interaction networks [22, 34-39]. Our work is a further development along the network decomposition approach [13, 14]. Our main contribution is to combine the global metric with a local metric in the decomposition procedure. We also resolved several critical technical issues. We propose (1) a new commonality metric based on random graph analysis, (2) a clear definition of protein modules utilizing the decomposition tree structure, and (3) a noise filtering algorithm based on random graph analysis. These advances in methodology result in an effective, consistent, and robust algorithm, as demonstrated on both simulated datasets and the experimental yeast interaction data. The protein modules obtained have clear biological functions, as shown in Table 5. Our approach to recover protein interaction modules is fully self-contained, i.e., it does not need other input or parameters to identify protein module boundaries. Our test experiments on yeast show that this method can effectively predict protein interaction modules from a complex interaction network. We plan to further automate this algorithm to compute protein interaction modules for a large number of organisms.

Materials and methods

Computing geometric accuracy and separation

We computed the geometric accuracy and separation by following the approach described in the study by Brohee and van Helden [16]. Briefly, each clustering result was compared with the annotated complexes by building a contingency table T, where row i corresponds to the ith annotated complex and column j to the jth cluster and the value of a

cell T_{ij} indicates the number of proteins found in common between complex i and cluster j. The contingency table has n rows (complexes) and m columns (clusters).

Accuracy. First, we define complex-wise sensitivity Sn_{co_i} as the maximal fraction of protein of complex i which could be found in one cluster by the formula $Sn_{co_i} = \max_{j=1}^{m}\left(T_{ij} / N_i\right)$, where N_i is the number of proteins belonging to complex i. To characterize the general sensitivity of a clustering result, we compute a clustering-wise sensitivity as the weighted average of Sn_{co_i} over all complexes by the formula $Sn = \frac{\sum_{i=1}^{n} N_i Sn_{co_i}}{\sum_{i=1}^{n} N_i}$.

Second, we calculate a cluster-wise positive predictive value PPV_{cl_j} as the maximal fraction of proteins of cluster j found in the best-matching complex by the formula $PPV_{cl_j} = \max_{i=1}^{n}\left(T_{ij} / T_{.j}\right)$, where $T_{.j}$ is the marginal sum of a column j by $T_{.j} = \sum_{i=1}^{n} T_{ij}$. To characterize the general PPV of a clustering result as a whole, we compute a clustering-wise PPV as the weighted average of PPV_{cl_j} over all clusters by $PPV = \frac{\sum_{j=1}^{m} T_{.j} PPV_{cl_j}}{\sum_{j=1}^{m} T_{.j}}$.

The geometric accuracy (Acc) indicates the tradeoff between sensitivity and predictive value. It is obtained by computing the geometric mean of the Sn and the PPV by $Acc = \sqrt{Sn \cdot PPV}$.

Separation. From the contingency table, we derive relative frequencies with respect to the marginal sums, either per row ($F_{row_{ij}} = \frac{T_{ij}}{\sum_{j=1}^{m} T_{ij}}$) or per column ($F_{col_{ij}} = \frac{T_{ij}}{\sum_{i=1}^{n} T_{ij}}$).

We then define the separation as the product of column-wise and row-wise frequencies by $Sep_{ij} = F_{col_{ij}} \cdot F_{row_{ij}}$. The complex-wise separation Sep_{co_i} is calculated as the sum of separation values for a given complex i by $Sep_{co_i} = \sum_{j=1}^{m} Sep_{ij}$ and the cluster-wise separation Sep_{cl_j} for cluster j by $Sep_{cl_j} = \sum_{i=1}^{n} Sep_{ij}$. To estimate a clustering result as a whole, complex-wise Sep_{co} and clustering-wise Sep_{cl} values are computed as the average of Sep_{co_i} over all complexes, and of Sep_{cl_j} over all clusters, respectively.

$$Sep_{co} = \frac{\sum_{i=1}^{n} Sep_{co_i}}{n}$$

$$Sep_{cl} = \frac{\sum_{j=1}^{m} Sep_{cl_j}}{m}$$

We then compute the geometric separation (Sep) as the geometric mean of Sep_{co} and Sep_{cl} by $Sep = \sqrt{Sep_{co} \cdot Sep_{cl}}$.

Acknowledgements

This research is supported by the program Molecular Assemblies, Genes, and Genomics Integrated Efficiently (MAGGIE) funded by the Office of Science, Office of Biological and Environmental Research, U.S. Department of Energy, under contract number: DE-AC02-05CH11231. We gratefully acknowledge Dr. Elizabeth Holbrook for editing this manuscript.

References

1. Eisen MB, Spellman PT, Brown PO, Botstein D: **Cluster analysis and display of genome-wide expression patterns**. *Proc Natl Acad Sci U S A* 1998, **95**(25):14863-14868.

2. Hughes TR, Marton MJ, Jones AR, Roberts CJ, Stoughton R, Armour CD, Bennett HA, Coffey E, Dai H, He YD *et al*: **Functional discovery via a compendium of expression profiles**. *Cell* 2000, **102**(1):109-126.

3. Ho Y, Gruhler A, Heilbut A, Bader GD, Moore L, Adams SL, Millar A, Taylor P, Bennett K, Boutilier K *et al*: **Systematic identification of protein complexes in Saccharomyces cerevisiae by mass spectrometry**. *Nature* 2002, **415**(6868):180-183.

4. Ito T, Tashiro K, Muta S, Ozawa R, Chiba T, Nishizawa M, Yamamoto K, Kuhara S, Sakaki Y: **Toward a protein-protein interaction map of the budding yeast: A comprehensive system to examine two-hybrid interactions in all possible combinations between the yeast proteins**. *Proc Natl Acad Sci U S A* 2000, **97**(3):1143-1147.

5. Krogan NJ, Cagney G, Yu H, Zhong G, Guo X, Ignatchenko A, Li J, Pu S, Datta N, Tikuisis AP *et al*: **Global landscape of protein complexes in the yeast Saccharomyces cerevisiae**. *Nature* 2006, **440**(7084):637-643.

6. Krogan NJ, Peng WT, Cagney G, Robinson MD, Haw R, Zhong G, Guo X, Zhang X, Canadien V, Richards DP *et al*: **High-definition macromolecular composition of yeast RNA-processing complexes**. *Mol Cell* 2004, **13**(2):225-239.

7. Gavin AC, Bosche M, Krause R, Grandi P, Marzioch M, Bauer A, Schultz J, Rick JM, Michon AM, Cruciat CM *et al*: **Functional organization of the yeast proteome by systematic analysis of protein complexes**. *Nature* 2002, **415**(6868):141-147.

8. Gavin AC, Aloy P, Grandi P, Krause R, Boesche M, Marzioch M, Rau C, Jensen LJ, Bastuck S, Dumpelfeld B *et al*: **Proteome survey reveals modularity of the yeast cell machinery**. *Nature* 2006, **440**(7084):631-636.

9. Tong AH, Lesage G, Bader GD, Ding H, Xu H, Xin X, Young J, Berriz GF, Brost RL, Chang M *et al*: **Global mapping of the yeast genetic interaction network**. *Science* 2004, **303**(5659):808-813.

10. Pan X, Ye P, Yuan DS, Wang X, Bader JS, Boeke JD: **A DNA integrity network in the yeast Saccharomyces cerevisiae**. *Cell* 2006, **124**(5):1069-1081.

11. Schuldiner M, Collins SR, Thompson NJ, Denic V, Bhamidipati A, Punna T, Ihmels J, Andrews B, Boone C, Greenblatt JF *et al*: **Exploration of the function and organization of the yeast early secretory pathway through an epistatic miniarray profile**. *Cell* 2005, **123**(3):507-519.

12. Hartwell LH, Hopfield JJ, Leibler S, Murray AW: **From molecular to modular cell biology**. *Nature* 1999, **402**(6761 Suppl):C47-52.

13. Girvan M, Newman ME: **Community structure in social and biological networks**. *Proceedings of the National Academy of Sciences of the United States of America* 2002, **99**(12):7821-7826.

14. Radicchi F, Castellano C, Cecconi F, Loreto V, Parisi D: **Defining and identifying communities in networks**. *Proceedings of the National Academy of Sciences of the United States of America* 2004, **101**(9):2658-2663.

15. Dongen Sv: **Graph Clustering by Flow Simulation**. University of Utrecht; 2000.

16. Brohee S, van Helden J: **Evaluation of clustering algorithms for protein-protein interaction networks**. *BMC bioinformatics* 2006, **7**:488.

17. Newman ME, Girvan M: **Finding and evaluating community structure in networks**. *Physical review* 2004, **69**(2 Pt 2):026113.

18. Mewes HW, Amid C, Arnold R, Frishman D, Guldener U, Mannhaupt G, Munsterkotter M, Pagel P, Strack N, Stumpflen V *et al*: **MIPS: analysis and annotation of proteins from whole genomes**. *Nucleic acids research* 2004, **32**(Database issue):D41-44.

19. Aiello W, Chung F, Lu L: **A random graph model for massive graphs**. In: *ACM Symposium on Thoery of Computing*. Portland, Oregon; 2000: 171-180.

20. Brandes U: **A Faster Algorithm for Betweenness Centrality**. *Journal of Mathematical Sociology* 2001, **25**(2):163-177.

21. Yang Q, Lonardi S: **A parallel edge-betweenness clustering tool for Protein-Protein Interaction networks**. *International Journal of Data Mining and Bioinformatics* 2007, **1**(3):241-247.

22. Spirin V, Mirny LA: **Protein complexes and functional modules in molecular networks**. *Proceedings of the National Academy of Sciences of the United States of America* 2003, **100**(21):12123-12128.

23. von Mering C, Krause R, Snel B, Cornell M, Oliver SG, Fields S, Bork P: **Comparative assessment of large-scale data sets of protein-protein interactions**. *Nature* 2002, **417**(6887):399-403.

24. Goldberg DS, Roth FP: **Assessing experimentally derived interactions in a small world**. *Proceedings of the National Academy of Sciences of the United States of America* 2003, **100**(8):4372-4376.

25. Samanta MP, Liang S: **Predicting protein functions from redundancies in large-scale protein interaction networks**. *Proceedings of the National Academy of Sciences of the United States of America* 2003, **100**(22):12579-12583.

26. Stark C, Breitkreutz BJ, Reguly T, Boucher L, Breitkreutz A, Tyers M: **BioGRID: a general repository for interaction datasets**. *Nucleic acids research* 2006, **34**(Database issue):D535-539.

27. Guldener U, Munsterkotter M, Oesterheld M, Pagel P, Ruepp A, Mewes HW, Stumpflen V: **MPact: the MIPS protein interaction resource on yeast**. *Nucleic acids research* 2006, **34**(Database issue):D436-441.

28. Boyle EI, Weng S, Gollub J, Jin H, Botstein D, Cherry JM, Sherlock G: **GO::TermFinder--open source software for accessing Gene Ontology information and finding significantly enriched Gene Ontology terms associated with a list of genes**. *Bioinformatics (Oxford, England)* 2004, **20**(18):3710-3715.

29. Li R: **Bifurcation of the mitotic checkpoint pathway in budding yeast**. *Proceedings of the National Academy of Sciences of the United States of America* 1999, **96**(9):4989-4994.

30. Wang A, Kurdistani SK, Grunstein M: **Requirement of Hos2 histone deacetylase for gene activity in yeast**. *Science (New York, NY* 2002, **298**(5597):1412-1414.

31. Roy N, Runge KW: **The ZDS1 and ZDS2 proteins require the Sir3p component of yeast silent chromatin to enhance the stability of short linear centromeric plasmids**. *Chromosoma* 1999, **108**(3):146-161.

32. Kallal LA, Bhattacharyya M, Grove SN, Iannacone RF, Pugh TA, Primerano DA, Clancy MJ: **Functional analysis of the sporulation-specific SPR6 gene of Saccharomyces cerevisiae**. *Current genetics* 1990, **18**(4):293-301.

33. Zheng Y, Cerione R, Bender A: **Control of the yeast bud-site assembly GTPase Cdc42. Catalysis of guanine nucleotide exchange by Cdc24 and stimulation of GTPase activity by Bem3**. *The Journal of biological chemistry* 1994, **269**(4):2369-2372.

34. Snel B, Bork P, Huynen MA: **The identification of functional modules from the genomic association of genes**. *Proceedings of the National Academy of Sciences of the United States of America* 2002, **99**(9):5890-5895.

35. Wilhelm T, Nasheuer HP, Huang S: **Physical and functional modularity of the protein network in yeast**. *Mol Cell Proteomics* 2003, **2**(5):292-298.

36. Xiong H, He X, Ding C, Zhang Y, Kumar V, Holbrook SR: **Identification of functional modules in protein complexes via hyperclique pattern discovery**. *Pacific Symposium on Biocomputing* 2005:221-232.

37. Bader GD, Hogue CW: **An automated method for finding molecular complexes in large protein interaction networks**. *BMC bioinformatics* 2003, **4**:2.

38. Bu D, Zhao Y, Cai L, Xue H, Zhu X, Lu H, Zhang J, Sun S, Ling L, Zhang N *et al*: **Topological structure analysis of the protein-protein interaction network in budding yeast**. *Nucleic acids research* 2003, **31**(9):2443-2450.

39. Chen J, Yuan B: **Detecting functional modules in the yeast protein-protein interaction network**. *Bioinformatics (Oxford, England)* 2006, **22**(18):2283-2290.

Figure legends

Figure 1 - A sample decomposition tree showing protein interaction modules

Special parents are marked with triangles. Modules as defined in the text are shaded subtrees. Two modules with the same parent are merged if the edge commonality between the two modules is above a threshold (shown as boxes). Dashed lines outline singletons.

Figure 2 - Robustness of the algorithms to random edge addition and removal

Each curve represents the value of accuracy (left panels) or separation (right panels). (A-B) edge addition to the test graph. (C-D) edge removal from an altered graph with 100% of randomly added edges. (E-F) edge addition to an altered graph with 40% of randomly removed edges. Color code: red: BCD, blue: GN, cyan: MCL, orange: ECC with the original edge clustering coefficient, green: ECC with our commonality index.

Figure 3 - A yeast transcriptional sub-network (upper) and the decomposition tree constructed by the BCD algorithm (lower)

Predicted protein modules are highlighted with colored bars (lower panel) and protein nodes in the network (upper panel) are colored accordingly. The module names in the upper panel are inferred from their members' annotation information. Singletons are colored red.

Figure 4 - Decomposition curves for the largest sub-networks of two datasets on unfiltered data (A) and filtered data (B) by the three algorithms

During the decomposition process, the larger connected component and the larger one of its derived sub-networks are always decomposed earlier. The y-axis shows the size of the

sub-network under decomposition and the x-axis shows the number of productive cuts so far. A productive cut means the removal of an edge splitting one network into two disconnected parts.

Figure 5 - Size distribution of predicted and MIPS protein complexes

Figure 6 - Examples of modules where the GO terms are greatly enriched

(A) A five-member module of the spindle-assembly checkpoint complex that is crucial in the checkpoint mechanism required to prevent cell cycle progression into anaphase in the presence of spindle damage. (B) A thirteen-member module including members (Set3, Hos2, Snt1, Hos4, Hst1, Sif2) from the Set3 histone deacetylase complex, proteins (Zds1, Zds2 and Skg6) involved in telomere silencing, proteins (Spr6 and Bem3) related to sporulation, and two other proteins (YIL055C and Cpr1).

Tables

Table 1 - Number of predicted complexes and singletons

Algorithm	Unfiltered		Filtered	
	Complex	Singleton	Complex	Singleton
BCD	850(5.0)	991	391(6.8)	361
GN	614(4.6)	2477	297(8.9)	379
ECC	875(3.5)	2214	491(4.1)	1021
MCL	703(7.3)	168	232(13.0)	3

The average size of complexes is shown in parentheses.

Table 2 - Comparison of modularity coefficients for network decomposition on three networks of varying sizes

Network	Size *n*	Modularity *Q*		
		BCD	GN	ECC
Transcription network	225	0.692	0.690	0.637
Filtered global data	3030	0.701	0.717	0.550
Unfiltered global data	5273	0.423	0.340	0.284

Table 3 - Comparison of predicted protein complexes with known MIPS complexes

Algorithm		BCD	GN	ECC	MCL
Unfiltered	100%[a]	59(6.9[b])	27(4.4)	56(6.4)	53(7.5)
	>50%	65(7.6)	51(8.3)	56(6.4)	63(9.0)
	>0%	125(14.7)	92(15.0)	122(13.9)	153(21.8)
	No overlap	601(70.7)	444(72.3)	641(73.3)	434(61.7)
	Accuracy[c]	0.70	0.64	0.62	0.65
	Separation[c]	0.21	0.16	0.20	0.27
Filtered	100%	53(13.6)	45(15.2)	50(10.2)	67(28.9)
	>50%	46(11.8)	38(12.8)	49(10.0)	24(10.3)
	>0%	83(21.2)	66(22.2)	120(24.4)	50(21.6)
	No overlap	209(53.5)	148(49.8)	272(55.4)	91(39.2)
	Accuracy	0.73	0.71	0.61	0.67
	Separation	0.29	0.28	0.26	0.38

[a]The overlap is defined as the percentage of proteins in the best-matching MIPS complexes in a predicted cluster. Complexes with only one protein are excluded in this analysis. [b]The percentage of total predicted protein complexes. [c]The geometric accuracy and separation according to the study[16].

Table 4 - Predicted protein complexes of size ≥ 3 enriched in GO terms

	Unfiltered				Filtered			
P	<e-15	e-15 – e-10	e-10 - e-5	e-5 - 1	<e-15	e-15 – e-10	e-10 – e-5	e-5 - 1
BCD	58(10.4)	41(7.4)	118(21.2)	339(61.0)	62(21.1)	38(13.0)	86(29.3)	108(36.7)
GN	47(24.1)	23(11.8)	43(22.1)	82(42.1)	60(24.4)	32(13.0)	66(26.8)	88(35.8)
ECC	47(10.1)	48(10.3)	120(25.9)	249(53.7)	45(13.7)	55(16.7)	114(34.7)	115(35.0)
MCL	55(11.2)	31(6.3)	96(19.6)	309(62.9)	55(24.1)	33(14.5)	62(27.2)	78(34.2)

The number in parentheses indicates the percentage of total complexes in that category.

Table 5 - Predicted protein modules where either GO terms are greatly enriched (P < 1e-15) or all members of a best-matching MIPS complex are found (overlap =100%)

Algorithm	Unfiltered(Percentage)	Filtered(Percentage)
BCD	95(11.2[b])	90(23.0)
GN	58(9.4)	80(27.0)
ECC	87(9.9)	83(16.9)
MCL	84(11.9)	91(39.2)

Additional files

Additional file 1 – Hierarchical decomposition trees of a yeast transcriptional sub-network by different algorithms

A PDF file (Sfigure1.pdf) of size 316KB

Additional file 2 – A list of predicted protein interaction modules by the BCD algorithm on the unfiltered dataset

A PDF file (Stable1.pdf) of size 1.8MB

Additional file 3 – A list of predicted protein interaction modules by the BCD algorithm on the filtered dataset

A PDF file (Stable2.pdf) of size 1.3MB

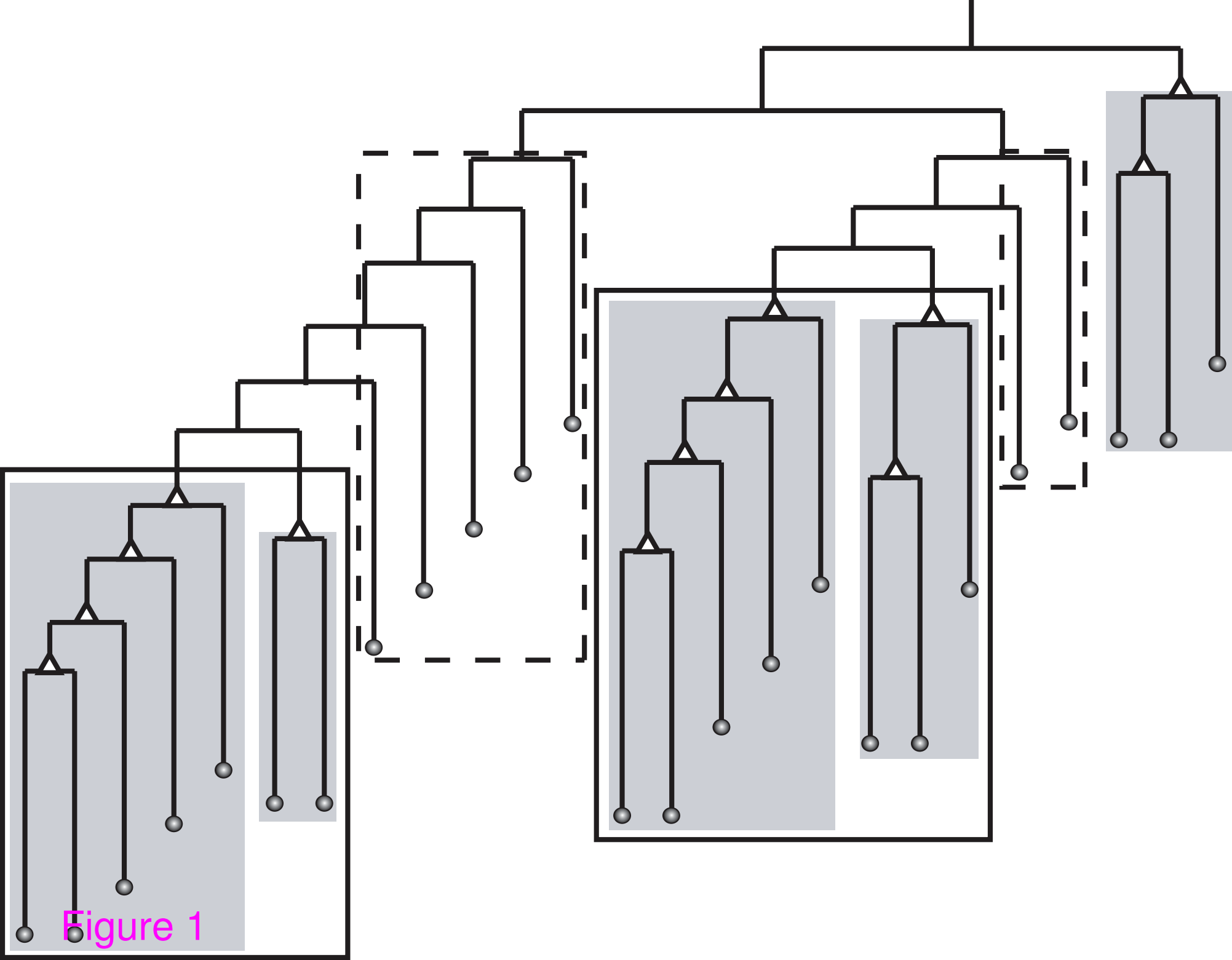
Figure 1

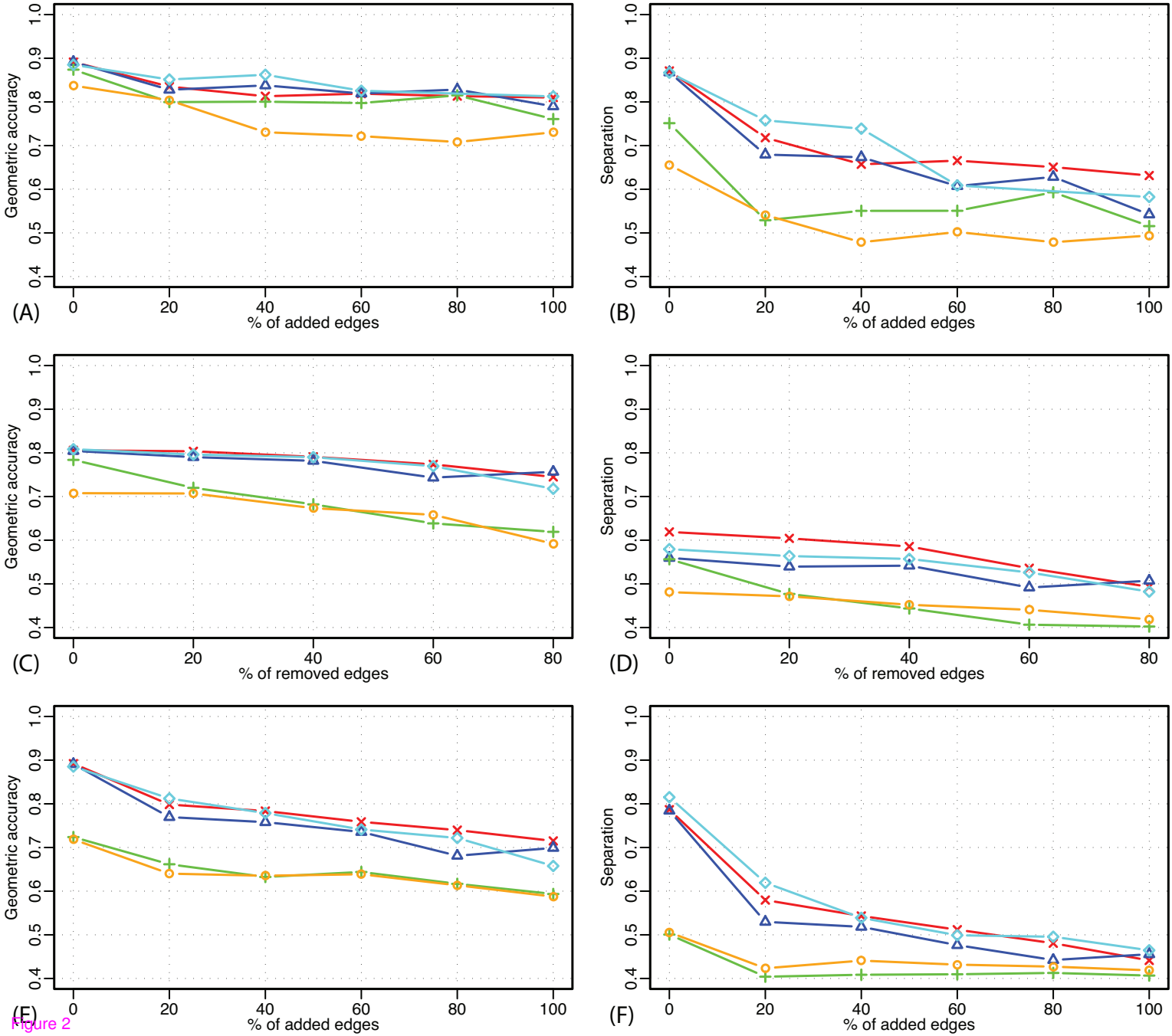
Geometric accuracy
Separation
% of added edges
% of removed edges
(A)
(B)
(C)
(D)
(E)
(F)

Figure 2

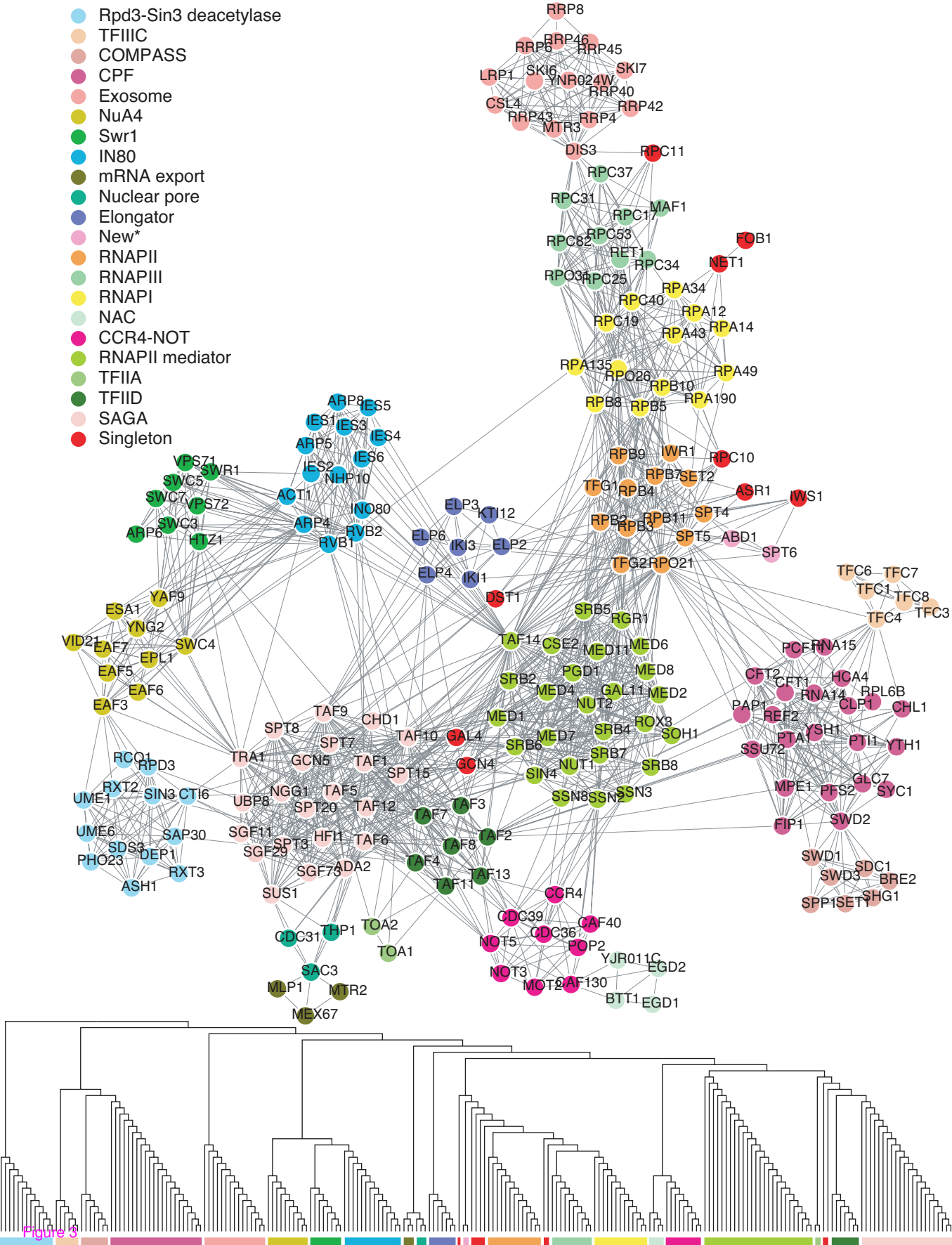
Rpd3-Sin3 deacetylase
TFIIIC
COMPASS
CPF
Exosome
NuA4
Swr1
IN80
mRNA export
Nuclear pore
Elongator
New*
RNAPII
RNAPIII
RNAPI
NAC
CCR4-NOT
RNAPII mediator
TFIIA
TFIID
SAGA
Singleton
RRP8
RRP46
RRP6
RRP45
LRP1
SKI6
SKI7
YNR024W
RRP40
CSL4
RRP42
RRP43
RRP4
MTR3
DIS3
RPC11
RPC37
RPC31
MAF1
RPC17
RPC53
RPC82
FOB1
RET1
RPC34
NET1
RPC31
RPC25
RPA34
RPC40
RPA12
RPC19
RPA43
RPA14
RPA135
RPO26
RPA49
RPB10
RPB8
RPB5
RPA190
ARP8
IES5
IES1
IES3
IES4
ARP5
IES6
IES2
NHP10
VPS71
SWR1
SWC5
SWC7
VPS72
ACT1
INO80
SWC3
ARP6
HTZ1
ARP4
RVB2
RVB1
ELP3
KTI12
ELP6
IKI3
ELP2
ELP4
IKI1
DST1
RPB9
IWR1
RPC10
RPB7
SET2
TFG1
RPB4
ASR1
IWS1
RPB2
RPB3
RPB11
SPT4
SPT5
ABD1
SPT6
TFG2
RPO21
TFC6
TFC7
TFC1
TFC8
TFC3
TFC4
YAF9
ESA1
YNG2
VID21
EAF7
SWC4
EPL1
EAF5
EAF6
EAF3
SRB5
RGR1
TAF14
CSE2
MED11
MED6
PCF11
RNA15
PGD1
MED8
SRB2
MED4
GAL11
MED2
CFT2
CFT1
HCA4
RNA14
RPL6B
NUT2
CLP1
CHL1
PAP1
REF2
TAF9
CHD1
MED1
ROX3
SPT8
SPT7
TAF10
GAL4
MED7
SRB4
SOH1
YSH1
PTA1
PTI1
YTH1
SSU72
RCO1
RPD3
TRA1
GCN5
TAF1
SRB6
SRB7
SPT15
GCN4
NUT1
SRB8
SIN4
RXT2
SIN3
CTI6
UME1
NGG1
TAF5
UBP8
SPT20
TAF12
SSN8
SSN2
SSN3
MPE1
PFS2
GLC7
SYC1
TAF3
TAF7
FIP1
SWD2
UME6
SAP30
SGF11
HFI1
TAF6
TAF2
SDS3
SPT3
TAF8
PHO23
DEP1
SGF29
ADA2
TAF4
SWD1
SDC1
RXT3
SGF73
TAF13
SWD3
BRE2
ASH1
TAF11
SUS1
CCR4
SPP1
SET1
SHG1
CDC39
CAF40
TOA2
THP1
CDC31
CDC36
NOT5
POP2
TOA1
YJR011C
EGD2
SAC3
NOT3
MLP1
MTR2
CAF130
BTT1
EGD1
MEX67

Figure 3

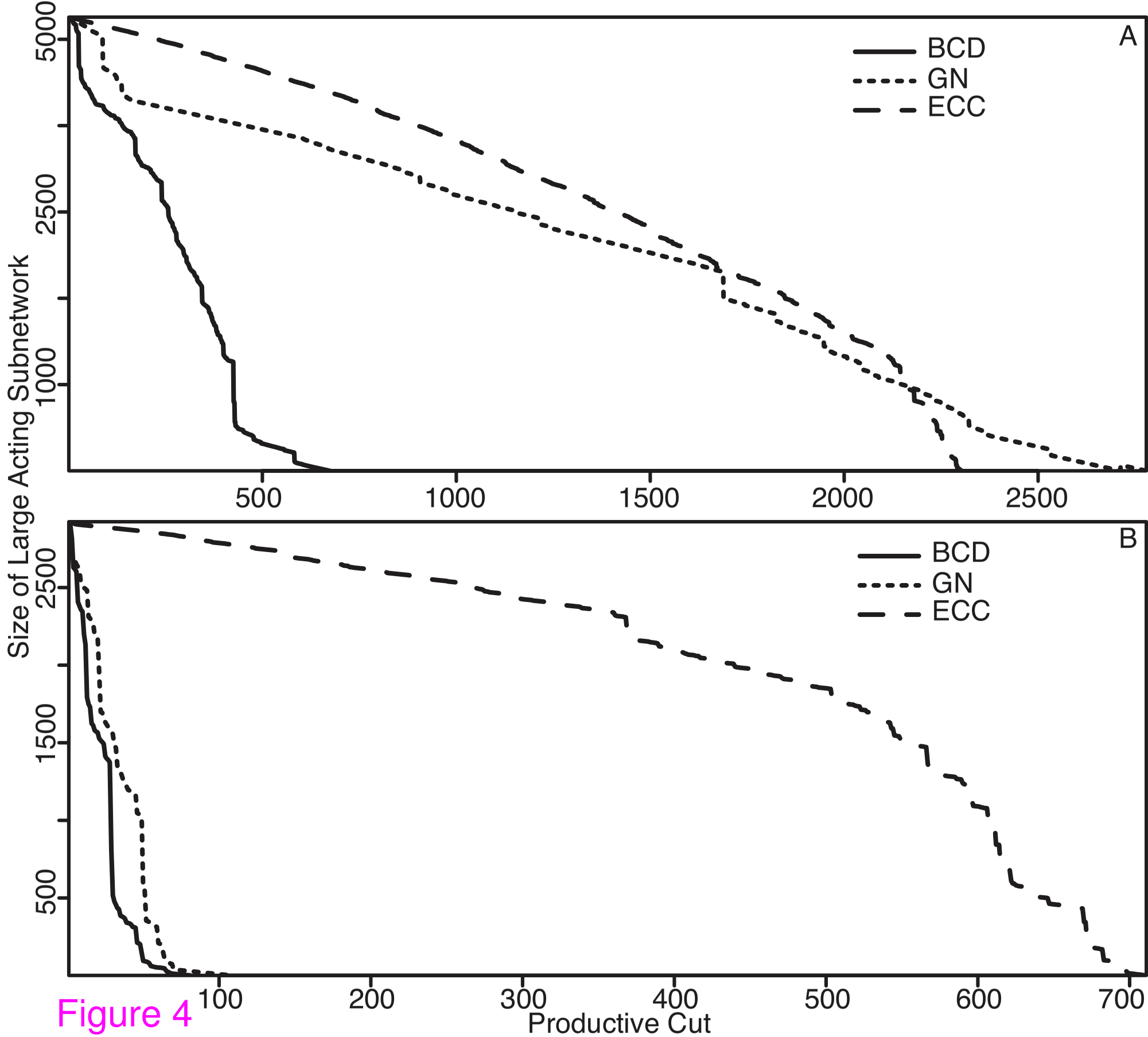
A
BCD
GN
ECC
5000
2500
1000
500
1000
1500
2000
2500
B
BCD
GN
ECC
2500
1500
500
100
200
300
400
500
600
700
Size of Large Acting Subnetwork
Productive Cut

Figure 4

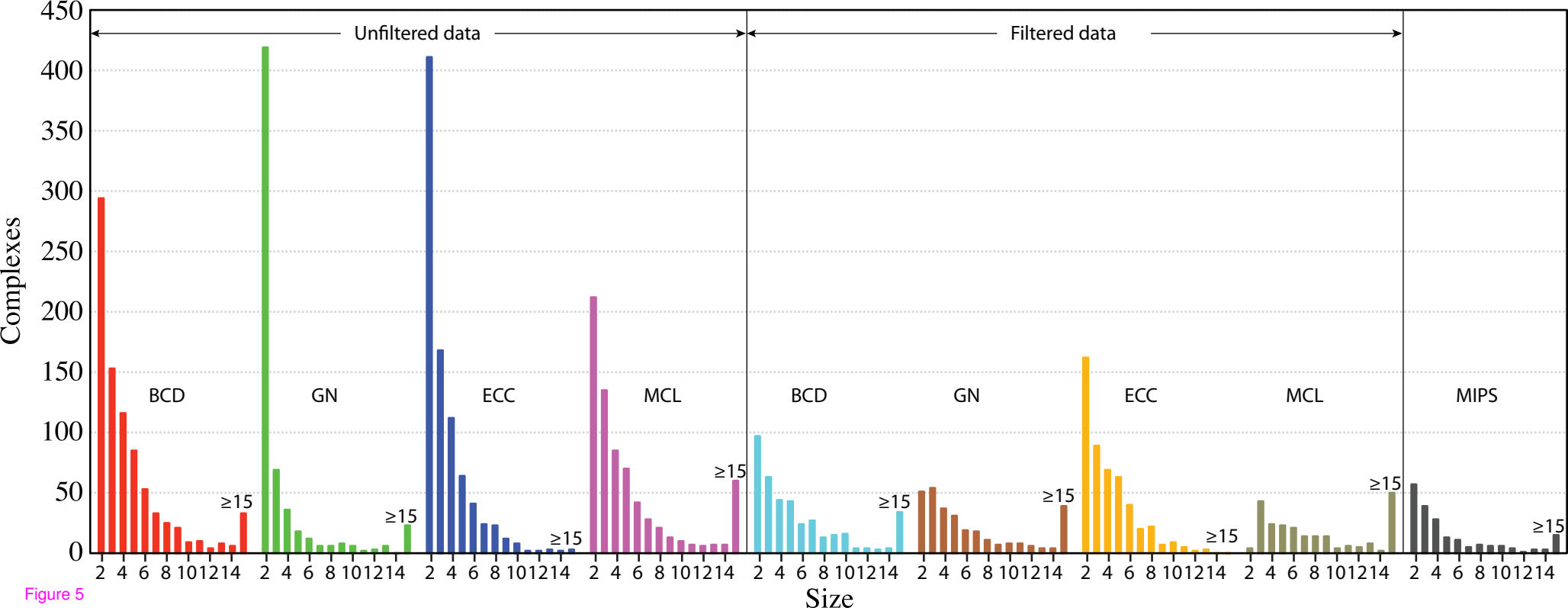
Unfiltered data
Filtered data
Complexes
Size
BCD
GN
ECC
MCL
BCD
GN
ECC
MCL
MIPS
≥15
0
50
100
150
200
250
300
350
400
450
2 4 6 8 10 12 14

Figure 5

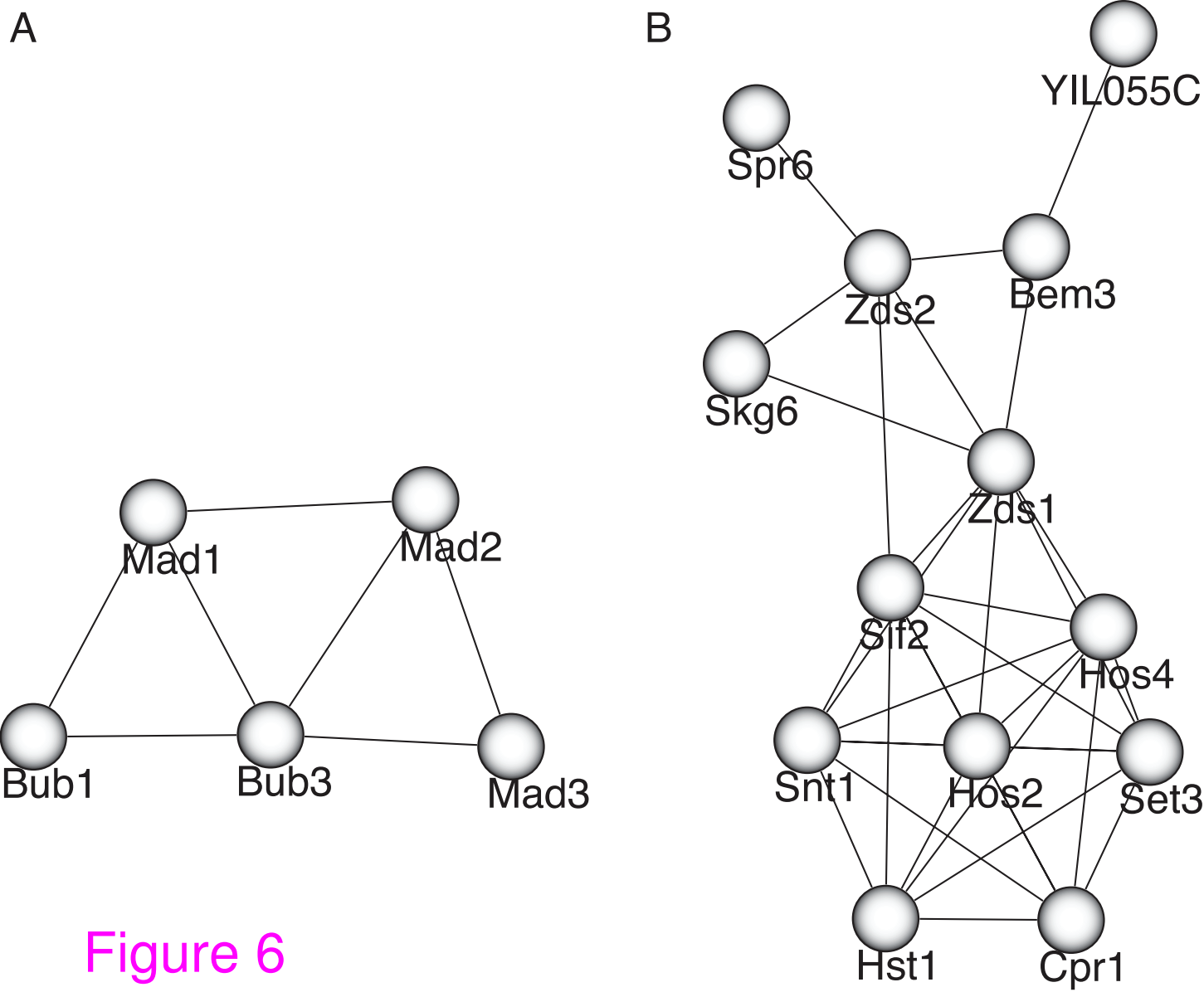
A
Mad1
Mad2
Bub1
Bub3
Mad3
B
YIL055C
Spr6
Zds2
Bem3
Skg6
Zds1
Slf2
Hos4
Snt1
Hos2
Set3
Hst1
Cpr1

Figure 6

Additional files provided with this submission:

Additional file 1: sfigure1.pdf, 300K
http://genomebiology.com/imedia/6832297591595134/supp1.pdf
Additional file 2: stable1.pdf, 1854K
http://genomebiology.com/imedia/1333514678149147/supp2.pdf
Additional file 3: stable2.pdf, 1327K
http://genomebiology.com/imedia/1502490411491474/supp3.pdf